International Journal of Environmental Science and Technology (2023) 20:5585–5596
https://doi.org/10.1007/s13762-022-04318-1

ORIGINAL PAPER

Experimental study on the adsorption and desorption performance of composite adsorbent activated carbon/calcium chloride

H. Zhao[1] · B. Zhang[1] · Y. Gao[1] · F. Zhang[1] · Y. Sun[1]

Received: 25 September 2021 / Revised: 1 February 2022 / Accepted: 24 May 2022 / Published online: 4 July 2022

Abstract

Facing the increasing shortage of fresh water resources in desert and arid areas, the adsorption water extraction method with adsorbent as water vapor carrier has attracted extensive attention of scholars. Although a large number of adsorbents for adsorption water intake method have been studied, it is still of practical significance to develop a simple and low-cost composite adsorbent for water intake process. A new composite adsorbent (activated carbon/calcium chloride) was synthesized by grinding with calcium chloride and activated carbon as raw materials. The micro-morphology of the composite adsorbent was observed by scanning electron microscope, and the water vapor adsorption and desorption properties of the composite adsorbent under different working conditions were measured. In addition, the adsorption kinetics and hydrothermal stability of the composite adsorbent were tested under specific working conditions. The experimental results show that the composite adsorbent shows good adsorption and desorption performance and good hydrothermal stability at low relative humidity. Therefore, the new composite adsorbent (activated carbon/calcium chloride) is expected to be applied in the adsorption water intake system.

Keywords Water harvesting · Composite adsorbent · Activated carbon · Calcium chloride · Adsorption and desorption performance

Introduction

With the over-exploitation and the pollution of water resources, the fresh water resources that we depend on for survival are gradually decreasing, especially in arid areas where fresh water resources are needed to solve the problems of living and production. Therefore, it is urgent to explore solutions to solve this problem. Currently, many scholars have done a lot of research work on desalination method, atmospheric air water generator, subsurface condensation method, fog collection method, and adsorption water extraction method (El-Ghonemy 2012; William et al. 2015; Kim et al. 2016; Srithar and Rajaseenivasan 2018; Salehi et al. 2020; Hanikel et al. 2020; Sharshir et al. 2020). Among the aforementioned water extraction methods, adsorption water extraction method has the advantage of not being restricted by geographical and climatic conditions. Therefore, it is considered as a feasible method for water extraction suitable for arid regions (Mohamed et al. 2017; Jarimi et al. 2020; Li et al. 2020). Meanwhile, the preparation of inexpensive adsorbents with good adsorption performance and cyclic stability is a key factor for the popularization of the adsorption water extraction method (Tu et al. 2018; Koc et al. 2020).

In recent years, zeolite has received extensive research as a matrix for synthesizing composite adsorbents with hygroscopic salts. Chan et al. (2012) studied the application of a composite adsorbent synthesized from 13X zeolite and $CaCl_2$ in a solar adsorption refrigeration system and investigated the effect of calcium ion exchange on the adsorption performance of 13X zeolite. The experimental results showed that the 13X/$CaCl_2$ composite adsorbent had better adsorption performance than the untreated 13X zeolite. Xu et al. (2019a) prepared a zeolite-$MgSO_4$ composite adsorbent using the impregnation method, and the results showed that the composite adsorbent had a stronger hydration capacity than pure zeolite, and increasing both the relative humidity and air temperature (< 50 °C) increased the saturation

---

Editorial responsibility: Samareh Mirkia.

✉ H. Zhao
hzzhao@shmtu.edu.cn

[1] Merchant Marine College, Shanghai Maritime University, Shanghai 201306, China

adsorption and hydration rate. Rehman et al. (2019) studied the water adsorption performance of $ZnSO_4$/13X zeolite composites under constant temperature and humidity, and the highest water absorption of the material reached 0.26 g/g, which was twice the adsorption capacity of pure ZnSO4-7H2O. Xu et al. (2018) developed a $MgSO_4$-impregnated 13X zeolite with activated alumina composite adsorbent for thermal storage. The adsorption and desorption characteristics of crude activated alumina and $MgSO_4$-impregnated activated alumina were studied and compared with the results of crude zeolite and $MgSO_4$-impregnated zeolite. Zhao et al. (2020a) synthesized a new composite adsorbent of LiCl + $CaCl_2$/13X, which showed the maximum adsorption capacity of CS6 reached 1.1 g/g at a temperature of 5 °C and 80% relative humidity and had good cyclic adsorption performance. In addition, new adsorbents based on silica gel as well as nanoporous materials compounded with hygroscopic salts have also received attention from scholars, and their sorption properties and applications have been studied. Tso et al. (2012) synthesized a composite adsorbent using activated carbon, silica gel and calcium chloride as raw materials, and established an adsorption isotherm and adsorption rate test device. The measured adsorption capacity was 0.23 kg/kg at 27 °C and water vapor pressure of 900 Pa. The use of multiple salts in adsorption refrigeration cycles has been extensively studied. Courbon et al. (2017) investigated silica gel composites loaded with CaCl2 and obtained a high cycle load of 0.40 g/g by a new synthetic scheme with 43 wt% $CaCl_2$ content in the composite enhancement. Entezari et al. (2018) impregnated two salts, LiCl and LiBr, in different ratios into silica gel pores and analyzed their tissue properties, water absorption isotherms and kinetics. The results showed that the molar ratio of the impregnated salts affected the adsorption characteristics. The addition of a small amount of LiBr to the LiCl composite can increase the adsorption capacity by 5.5%, while the addition of LiCl to the LiBr composite can decrease the adsorption capacity by 12.7%. As the field of air extraction continues to be explored, metal organic frameworks (MOFs) have attracted the attention of scholars (Oladoye et al. 2021). Mesgarian et al. (2020) synthesized UiO-66(NH2) nanosorbents, and it was found that higher regeneration and drying efficiency were obtained compared to silica gel, activated alumina and zeolite. Zhao et al. (2020b) conducted an in-depth study of MIL-101(cr) synthesized with sodium acetate as the mineralizing agent and reported the water adsorption performance of this adsorbent. Meanwhile, Zhao et al. (2020b) synthesized LiCl-modified UiO-66 composite adsorbent by impregnation method and found that the addition of LiCl enhanced the water adsorption performance of the composite adsorbent by open-form adsorption performance test. Activated carbon and activated carbon fibers have well-developed pore volume, high specific surface area and good thermal stability and have been widely used as substrates for adsorbents and composite adsorbents. Ye et al. (2014) investigated activated carbon fiber cloth (ACFC) and $CaCl_2$ composite adsorbent (CS) prepared by impregnation method. The experimental results showed that CSs with 15.2% and 22.8% $CaCl_2$ content had greater water absorption than the same amount of $CaCl_2$ and the performance index of the air conditioning cycle calculated from the isomers of CS containing the maximum $CaCl_2$ content could reach 0.7, which was considered suitably for adsorption refrigeration. Wang et al. (2016) developed a $CaCl_2$ matrix and a new composite adsorbent with activated carbon fiber mat (ACF mat) as the matrix. It was shown that ACF was more suitable as a matrix for composite adsorbent than silica matrix composite adsorbent, and ACF30 had the best water absorption performance with 1.7 g/g, which was three times higher than that of silica-$CaCl_2$. Yu et al. (2019) prepared a walnut shell activated carbon (AC0) using KOH chemical activation method and used it as a substrate for impregnation with the hygroscopic salt $MgCl_2$. And the effects of $MgCl_2$ loading and Ce addition on the water vapor adsorption performance of the composite adsorbent were investigated. The results showed that the water vapor adsorption performance of the adsorbent decreased slightly and then increased significantly with increasing $MgCl_2$ loading, and the addition of Ce improved the adsorption regeneration performance. Huang et al. (2021) prepared a series of activated carbon fiber (ACF)-based adsorbents for water vapor adsorption behavior using low-temperature plasma technology (LTOP) as a surface modification method. The study presented the conclusion that the adsorption performance of the LTOP-treated ACF was enhanced.

Most of the aforementioned preparation of composite adsorbents require a lot of time, and the preparation process is relatively complex. Compared with the above-mentioned preparation schemes, the process of preparing composite adsorbents by grinding and mixing is simpler and the experimental materials are easier to prepare. Zhang et al. (2015) prepared a new $CaCl_2$/MWNT adsorbent using carbon nanotubes as the matrix and a simple mixing method, and the experiment showed that a part of $CaCl_2$ was adsorbed on the surface of the matrix in the composite and the rest of the hygroscopic salt filled in the space of the matrix. The nanoparticles with large specific surface area can fully contact with water vapor and improve the adsorption rate of the water. However, due to the complicated process of making multi-walled carbon nanotubes, the production cost is high. Therefore, in this experiment, calcium chloride ($CaCl_2$) with good hygroscopic effect and inexpensive activated carbon (AC) were selected as raw materials to synthesize the composite adsorbent $CaCl_2$/AC (ACL) using the grinding and mixing method. In addition, the adsorption process of composite adsorbent is divided into physical adsorption and chemical adsorption. Physical adsorption refers to the rapid occupation of the pore structure of the composite adsorbent by water molecules, and this process proceeds relatively quickly. Chemisorption mainly refers to the absorption of water molecules by hygroscopic salts, and this process proceeds more slowly. AC has a high specific surface area and a well-developed pore structure, which can effectively prevent the dampness of the composite adsorbent in the adsorption process, and is the preferred material for synthetic composite adsorbents. The composite adsorbent was characterized by scanning electron microscopy (SEM). Under the experimental conditions of open adsorption, the composite adsorbent exhibited good adsorption/desorption performance. In addition, the cycling stability of the composite adsorbent was tested under specific working conditions, and the experimental results showed that the composite adsorbent has good cycling stability, which is an important condition for the application of the composite adsorbent. The new composite adsorbent proposed in this paper has advantages in production process and material cost, and can obtain good adsorption performance at low ambient humidity. Therefore, it is expected to be applied in the adsorption water extraction schemes in deserts and arid regions. This experiment was conducted in Shanghai, China, from December 2020 to July 2021.

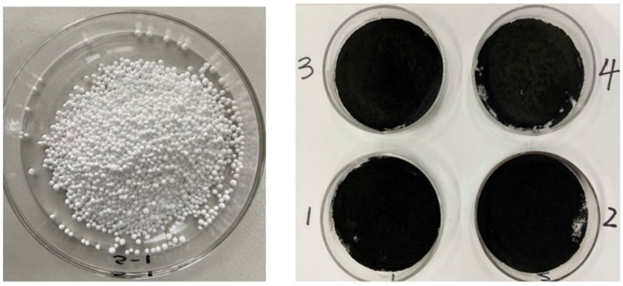

(a) (b)

Fig. 1 Physical diagram of experimental raw materials. **a** Anhydrous calcium chloride granules; **b** composite adsorbent samples

Materials and methods

Experimental raw materials and instruments used

The raw materials used in the experiment include: activated carbon (powder), analytical pure, produced by Fuchen (Tianjin) Chemical Reagent Co., Ltd; anhydrous calcium chloride is shown in Fig. 1a, analytical pure AR, Item No.: st10068-500 g, white particles, calcium chloride content ≥ 96%, provided by Collins experimental product supplier.

The instruments used in the experiment include: constant temperature and humidity box, which is produced by Shanghai Yiheng Scientific Instrument Co., Ltd; the electric heating constant temperature blast drying oven is produced by Tianjin Tonglixinda instrument factory; Electronic balance; Digital scanning electron microscope, produced by Beijing Zhongke Scientific Instrument Co., Ltd.

Preparation of composite adsorbents

The preparation process of the composite adsorbents is shown in Fig. 2.

1. The dried petri dish was placed on an electronic balance to weigh the appropriate amount of AC, and the beaker with the activated carbon was put into an electric heating constant temperature blast drying oven, and the temperature of the drying oven was set to 110 °C for drying for 4 h to remove the water vapor and other impurities in the AC.
2. $CaCl_2$ comprising 25%, 30%, 35% and 40% of the mass fraction of the composite adsorbents was mixed with the dried AC in a mortar for thorough grinding, defined as ACL25, ACL30, ACL35 and ACL40, respectively.
3. The ground samples were put into the pre-numbered dry Petri dishes as shown in Fig. 1b, and then, the Petri dishes were put into the drying oven at 110 °C until the sample mass no longer changed, and the composite adsorbents were considered to be prepared successfully.

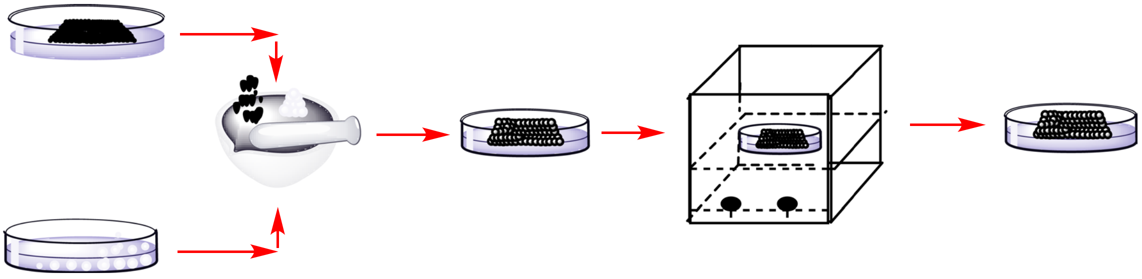

Fig. 2 Compound adsorbent ACL preparation flow chart

Results and discussion

Physical characterization of the composite adsorbents

As shown in Fig. 3a and b, the SEM images of AC raw powder and anhydrous calcium chloride were used to characterize the microstructure of the composite adsorbents, and it can be seen from the figures that AC raw powder and anhydrous calcium chloride were sparsely distributed and no accumulation phenomenon occurred. Figure 3c–f indicates the SEM images of ACL25, ACL30, ACL35, and ACL40, respectively, and it can be observed that the aggregation of the adsorbents becomes more and more obvious with the increase in the salt content of the composite adsorbents. From the SEM images of Fig. 3c and d, it can be seen that a small portion of the activated carbon particles in the composite adsorbents are wrapped by the hygroscopic salt, but still has a more developed structure and a higher specific surface area. From Fig. 3e and f, it can be seen that most of the activated carbon is wrapped by the hygroscopic salt, which means that the developed structure and specific surface area of the composite adsorbents are destroyed.

Adsorption and desorption performance test of the composite adsorbents

The adsorption and desorption performance of the composite adsorbent is an important indicator of the performance of the adsorbent. In order to investigate the adsorption and desorption characteristics of the composite adsorbent ACL, the appropriate temperature and humidity were screened

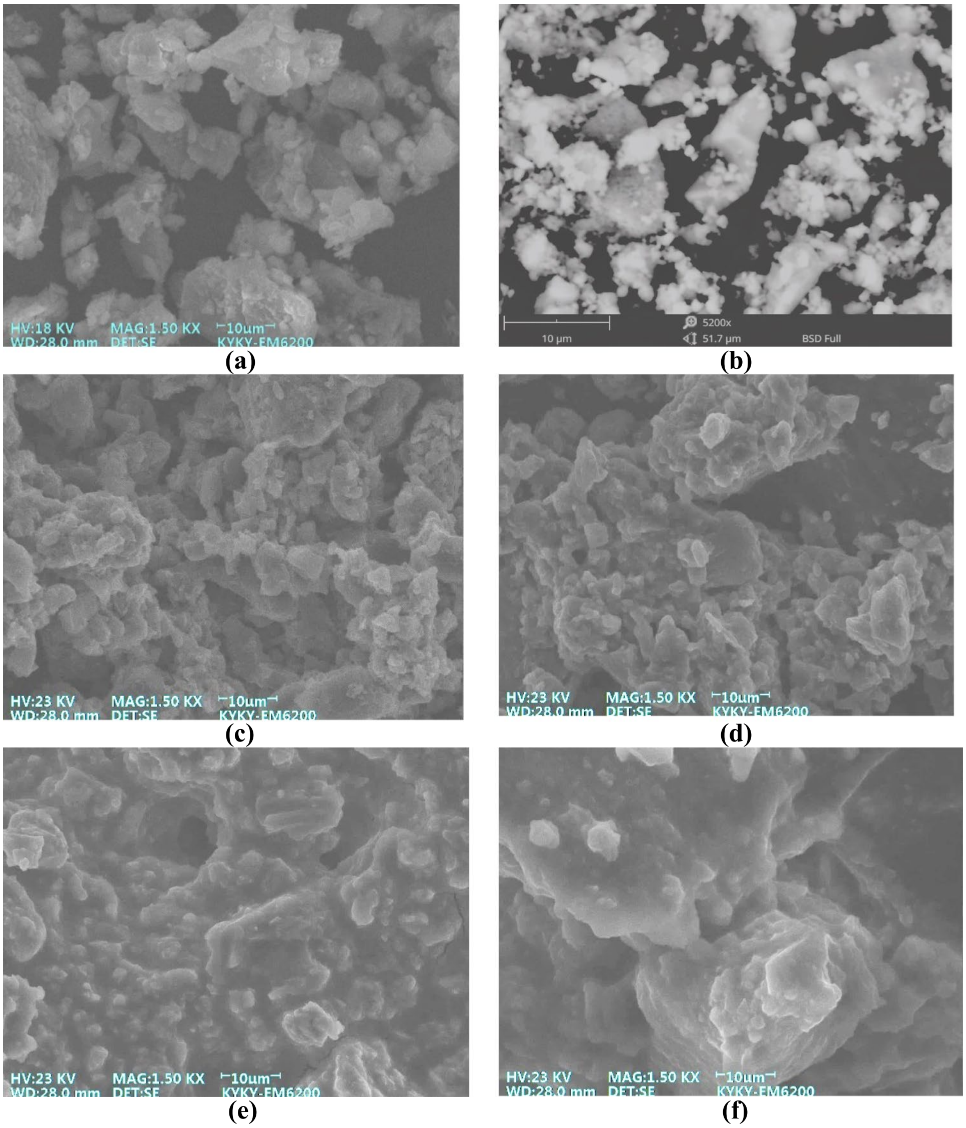

(a) (b) (c) (d) (e) (f)

Fig. 3 SEM image. **a** SEM image of AC; **b** SEM images of calcium chloride; **c** SEM images of ACL25; **c** SEM images of ACL30; **d** SEM images of ACL35; **e** SEM images of ACL40 to obtain a better adsorption and desorption effect for better application in the actual air extraction of water. The adsorption and desorption performance of the composite adsorbents with mass fractions of 25%, 30%, 35% and 40% (ACL25, ACL30, ACL35 and ACL40) was tested in a constant temperature and humidity chamber. The adsorption performance of the adsorbents was tested from 0 to 3 h at 15-min intervals, from 3 to 6 h at 30-min intervals, and after 6 h at 1-h intervals until saturation.

Adsorption and desorption performance test at 25 °C and 45% RH

As shown in Fig. 4, the adsorption rate of the four different salt content composite adsorbents was high in the first 3 h of the experiment at 25 °C and 45% humidity. This is because the composite adsorbents have a well-developed pore structure as well as a high specific surface area, which helps to improve the adsorption performance (Chan et al. 2015); in addition, the increase in salt content intensifies the chemisorption process between water molecules and adsorbent, and water molecules can be absorbed more by the composite adsorbents (Zhang et al. 2018; Xu et al. 2019b). At this time, the adsorption amounts of ACL25, ACL30, ACL35, and ACL40 reached 85%, 77.94%, 72.85%, and 72.19% of the equilibrium adsorption amounts, respectively. It can be seen that the more salt content and the less activated carbon content, the greater the difference between the composite adsorbents and the equilibrium adsorption amount. This is because as the salt content increases, the composite adsorbents exhibit agglomeration, which leads to a significant reduction in the contact area between the adsorbents and water vapor, resulting in a decrease in the adsorption rate (Zhang et al. 2015). This is consistent with the microscopic pattern changes observed in the SEM images of the composite adsorbents. After the experiment was conducted for 10 h, the salt content ACL25 composite adsorbent adsorption equilibrium, and the adsorption amounts of ACL30, ACL35, and ACL40 composite adsorbents reached 97.06%, 97.35%, and 96.45% of the equilibrium adsorption amounts, respectively. The experiments were carried out for 14 h and all the composite adsorbents were adsorbed in equilibrium, and the equilibrium adsorption amounts were 0.4027 g/g, 0.4503 g/g, 0.4903 g/g, 0.5578 g/g. The experimental results showed that the adsorption capacity of the composite adsorbents increased with the increase in the salt content of the composite adsorbents, and the composite adsorption capacity of ACL40 was about 1.39 times of that of ACL25.

As shown in Fig. 5, the desorption performance of the composite adsorbents was tested under the desiccator temperature of 110 °C. The experimental results showed that the four adsorbents with different salt contents showed good desorption performance at 110 °C, and the desorption experiments were carried out for 120 min and the composite adsorbents reached desorption equilibrium, and the resolution rates of ACL25, ACL30, ACL35 and ACL40 were 96.67%, 97.06%, 96.69% and 96.45%, respectively. In addition, after the experiment was conducted for 15 min, the desorption of the four composite adsorbents reached 88.33%, 84.56%, 70.86%, and 66.86% of the total adsorbed amount, respectively; this is because as the salt content increases and the activated carbon content decreases, the thermal conductivity of the composite adsorbents decreases, and so does the desorption rate.

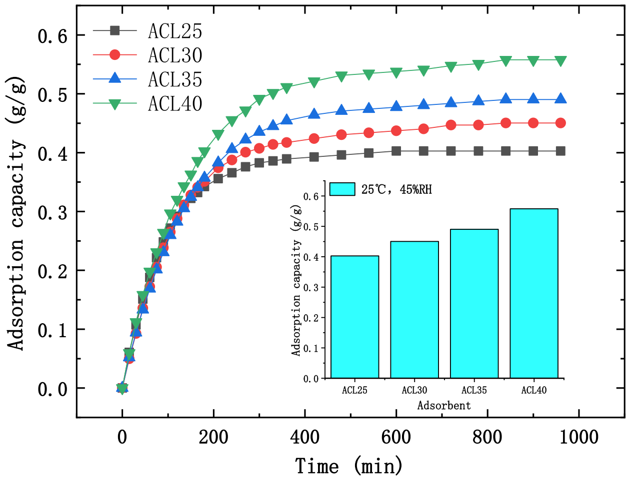

Fig. 4 Adsorption performance of composite adsorbent 25 °C, 45% RH

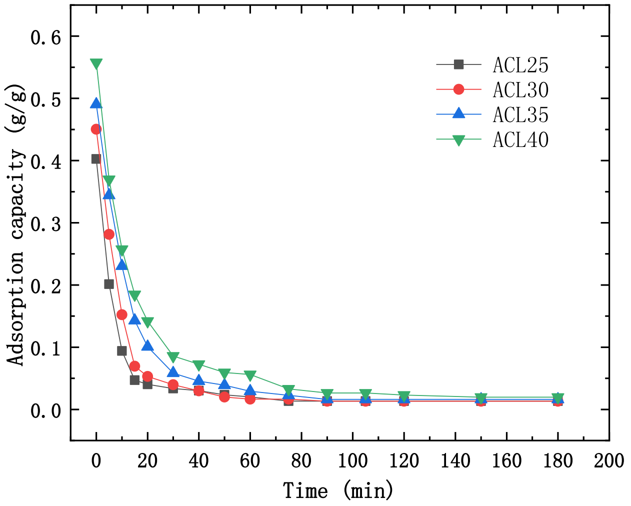

Fig. 5 Desorption performance of composite adsorbents at 25 °C and 45% RH

Analysis of water vapor adsorption and desorption performance of composite adsorbents at specific temperature

As shown in Fig. 6, the adsorption performance tests were performed at 25 °C in constant temperature and humidity chamber with relative humidity of 35%, 45% and 55% working conditions, respectively. The experimental results showed that the adsorption amount of the composite adsorbent increased with the increase in salt content when the humidity varied from 35 to 55% under the ambient temperature of 25 °C working condition; in addition, the adsorption amount of the composite adsorbents increased with the increase in humidity under the working condition of 25 °C. The adsorption of ACL40 at 55% RH reached a maximum of 0.6689 g/g, which was 1.52 times higher than that of ACL40 at 35% RH.

As shown in Fig. 7, the desorption data of the composite adsorbents at 110 °C after completion of adsorption at 25 °C in a constant temperature and humidity chamber with relative humidity of 35%, 45%, and 55%, respectively. It can be seen from the figure that the composite adsorbents with different salt contents showed good desorption performance under several conditions of 35%, 45% and 55% relative humidity, and the desorption rate reached between 94 and 99%.

Analysis of water vapor adsorption and desorption performance of composite adsorbents under specific humidity

As shown in Fig. 8, the adsorption performance of the composite adsorbents was tested under the humidity control of 45% RH and the temperature of 15 °C, 25 °C and 35 °C, respectively. The experimental results showed that: (1) the

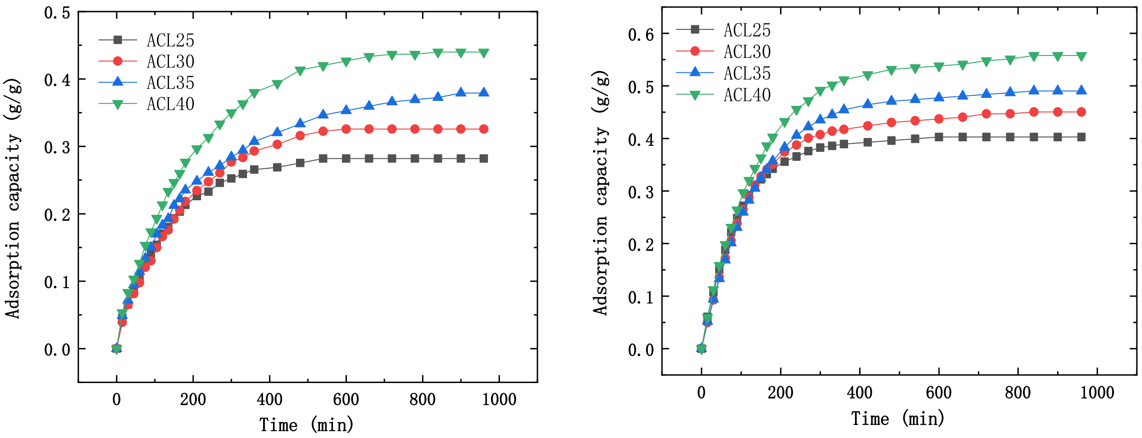

(a) 25℃, 35%RH adsorption **(b)** 25℃, 45%RH adsorption

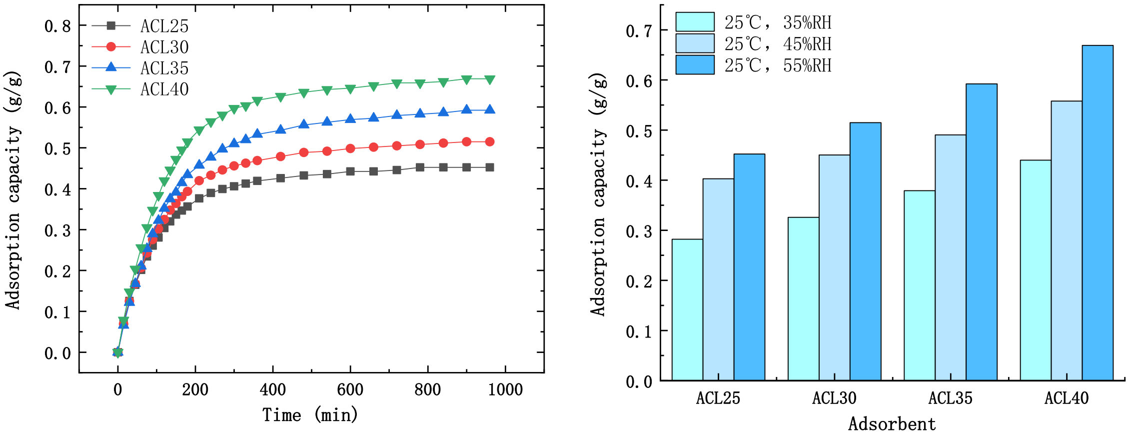

(c) 25℃, 55%RH adsorption **(d)** Comparison of adsorption performance in 25°C working condition

Fig. 6 Adsorption performance of composite adsorbents at 25 °C working condition

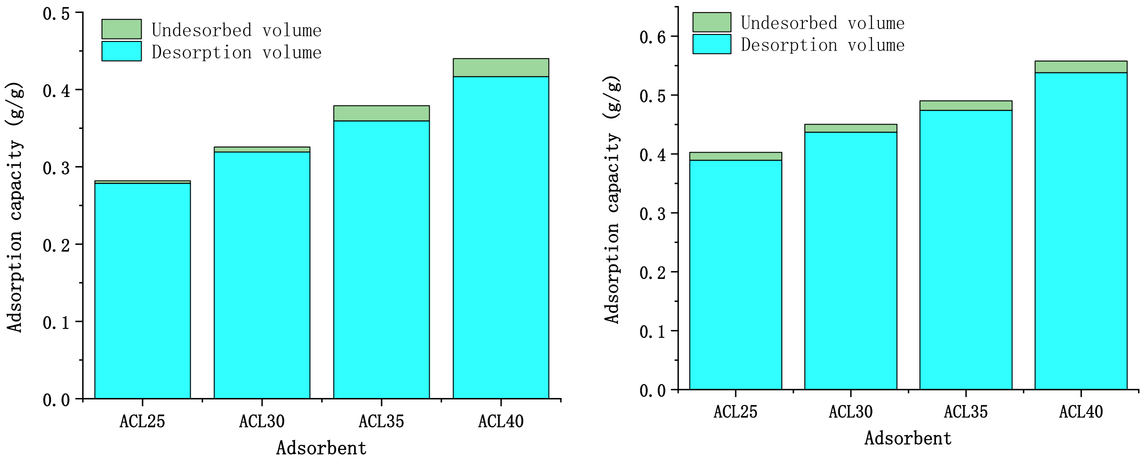

(a) 25℃, 35%RH desorption **(b)** 25℃, 45%RH desorption

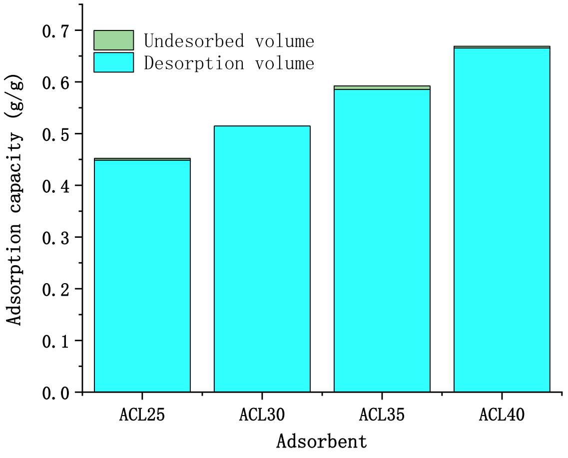

(c) 25℃, 55%RH desorption

Fig. 7 Desorption performance diagram of composite adsorbents at 110 °C

adsorption capacity of the composite adsorbents increased with the increase in salt content under all three conditions. (2) The adsorption capacity of ACL25, ACL30, ACL35 and ACL40 reached more than 90% of the equilibrium adsorption capacity after 3 h of the experiments at 35 °C and 45% RH, and the adsorption rate was significantly increased compared with that at 15 °C, 25 °C and 45% RH; in addition, under 35 °C and 45% RH conditions, the composite adsorbents reached adsorption equilibrium after 6 h, which was 1.83 times shorter than that under 15 °C and 45% RH conditions, and 1.33 times shorter than that under 25 °C and 45% RH conditions. The reason for this is that the increase in temperature increases the water vapor partial pressure, which accelerates the binding rate of water molecules to the composite adsorbent. (3) As shown in Table 1, the equilibrium adsorption capacities of ACL25, ACL30, ACL35 and ACL40 were 0.3523 g/g, 0.4139 g/g, 0.4554 g/g and 0.5049 g/g at 15 °C and 45% RH, respectively; 0.4027 g/g, 0.4503 g/g, 0.4903 g/g and 0.5578 g at 25 °C and 45% RH, respectively; 0.3754 g/g, 0.4257 g/g, 0.4869 g/g and 0.5516 g/g at 35 °C and 45% RH, respectively. The adsorption capacity of the four composite adsorbents increased by about 10% at 25 °C compared with that at 15 °C; the adsorption capacity of the four composite adsorbents decreased slightly at 35 °C compared with that at 25 °C. The reason is that the effect of temperature increase on the increase in water vapor partial pressure is higher than the effect of heat of adsorption of composite adsorbents in the adsorption process in the 15 °C working condition compared with the 25 °C working condition, which leads to the increase in adsorption capacity of composite adsorbents in the 25 °C working condition compared with the 15 °C working condition. At 35 °C compared to 25 °C, the effect of increasing temperature on the partial pressure of water vapor at the beginning of the experiment leads to an increase in the adsorption rate of the composite adsorbents. However, since

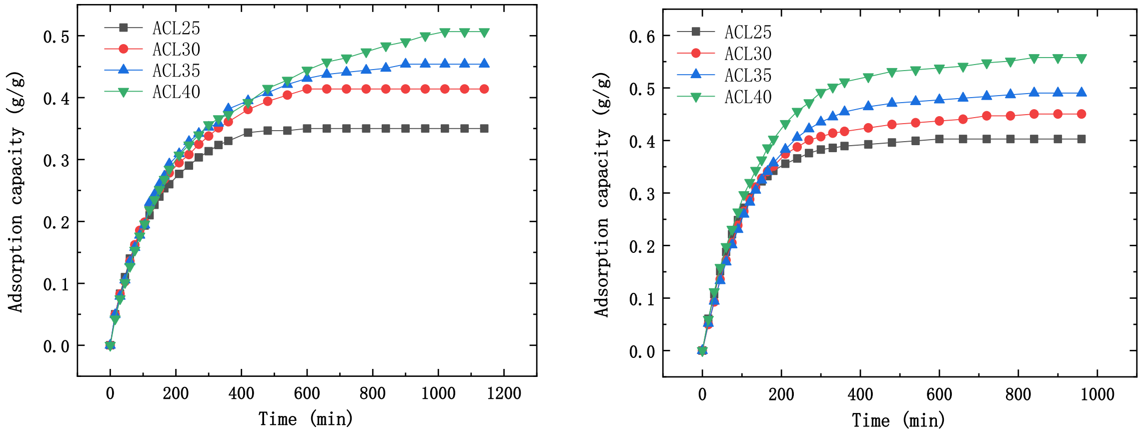

(a) 15℃, 45%RH adsorption

(b) 25℃, 45%RH adsorption

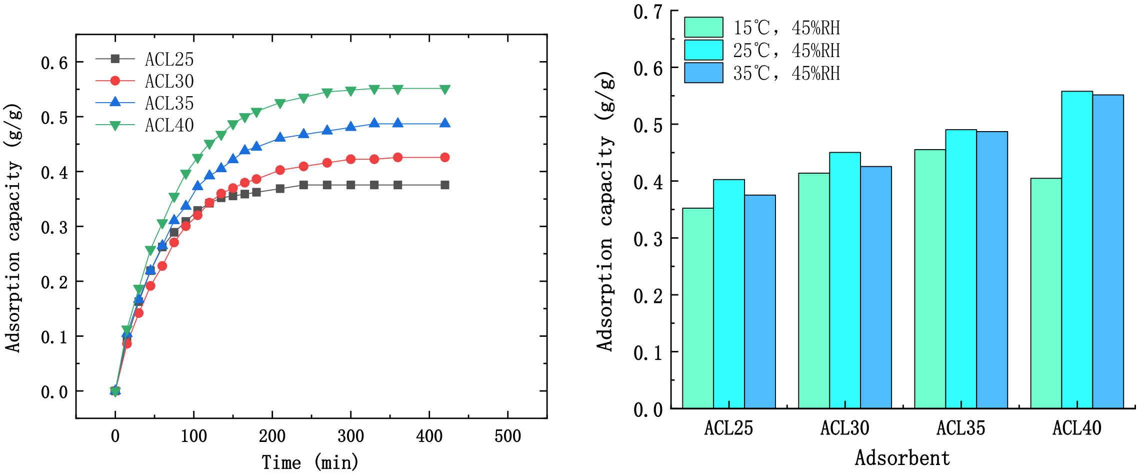

(c) 35℃, 45%RH adsorption

(d) Comparison of adsorption performance in 45%RH working condition

Fig. 8 Adsorption performance of the composite adsorbents at 45% RH working condition

Table 1 Adsorption data of composite adsorbents at 45% RH

	Working condition		
Samples	45%RH, 15 °C	45%RH, 25 °C	45%RH, 35 °C
ACL25	0.3523	0.4027	0.3754
ACL30	0.4139	0.4503	0.4257
ACL35	0.4554	0.4903	0.4869
ACL40	0.5049	0.5578	0.5516

the adsorption process of the composite adsorbents includes both physical and chemical adsorption, the adsorption process releases the heat of adsorption as the experiment proceeds. Because the faster the adsorption rate, the more intense the chemisorption process proceeds, more heat of adsorption is generated, which suppresses the adsorption capacity of the composite adsorbents and eventually leads to a decrease in the adsorption capacity at 35 °C compared to 25 °C.

Figure 9 shows the desorption diagram of the composite adsorbents at 110 °C after the adsorption is completed at 45% RH and the temperatures are 15 °C, 25 °C and 35 °C, respectively. From the comparison of the desorbed and undesorbed amounts, it can be found that the composite adsorbents exhibited good desorption performance with a desorption rate of more than 96%.

Analysis of the cycling performance of the composite adsorbents

The cycling stability performance of the composite adsorbent is an important indicator of whether the composite adsorbent can be used in practical water extraction applications. The following experimental study was conducted on

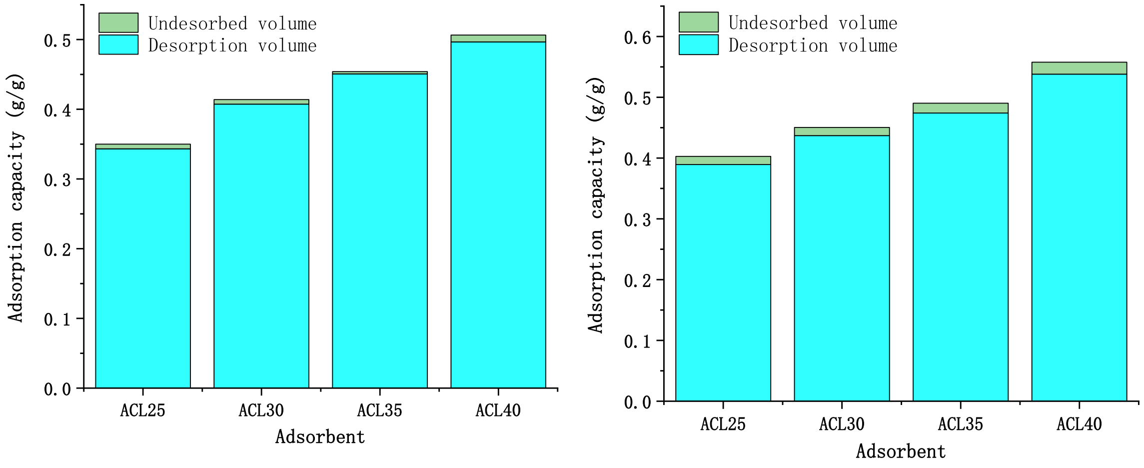

(a) 15℃, 45%RH desorption

(b) 25℃, 45%RH desorption

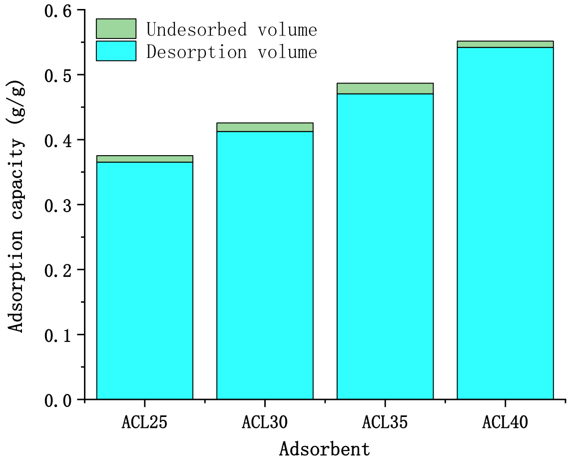

(c) 35℃, 45%RH desorption

Fig. 9 Desorption performance of composite adsorbents 45% RH working condition

the cyclic stability performance of the composite adsorbent ACL. Six cycles of adsorption and desorption tests were conducted on four different salt content composite adsorbents at 25 °C and 45% humidity, and the cyclic performance is shown in Fig. 10. The results showed that ACL25, ACL30, and ACL35 had good cycling stability, but ACL40 showed deliquescence during the cycle test. As shown in Fig. 11, the salt in the ACL40 composite adsorbent cannot be stably attached around the activated carbon to form a stable structure, thus causing the salt solution to flow out, so ACL40 is not suitable for practical application under this condition, and ACL35 should be selected as a better choice.

Adsorption kinetics fitting

For solar air water extraction systems, the adsorption kinetics cannot be neglected when considering vapor absorption in a specific environment. It can be seen from Fig. 12 that at the beginning of the experiment as a fast water uptake phase, the composite adsorbents has a high adsorption rate, and as time goes on, the fitted curve flattens out and the adsorption rate slows down until the composite adsorbents reach adsorption equilibrium. Again, it can be seen that the water vapor adsorption of the composite adsorbents is related to the salt content. The water vapor adsorption with time for the four composite adsorbents with different salt contents used in this experiment can be modeled using a quasi-first-order model (Eq. (1), Table 2) (Sun et al. 2020). This model has a wide range of applicability and can be used to study the adsorption rates of the adsorbents.

$$q_t = q_e\left(1 - e^{-kt}\right) \tag{1}$$

where q_e represents the equilibrium sorption (mg/g), q_t represents the dynamic sorption (mg/g), k represents the rate coefficient (s^{-1}), and t represents the time (s). Figure 12

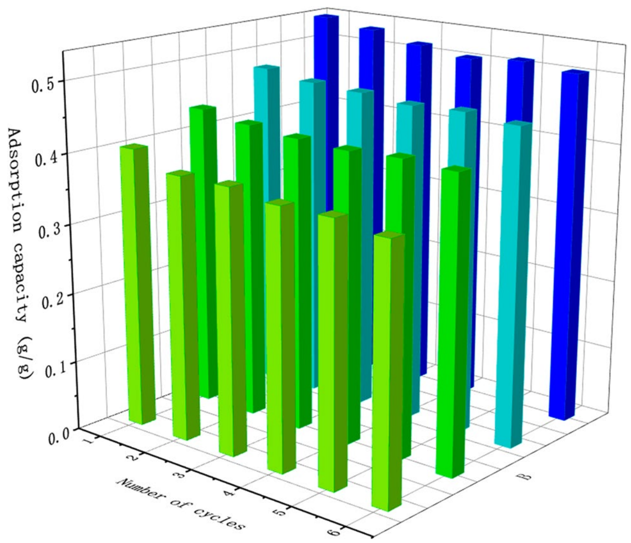

Fig. 10 Composite adsorbents 25 °C, 45% RH cycle performance graph

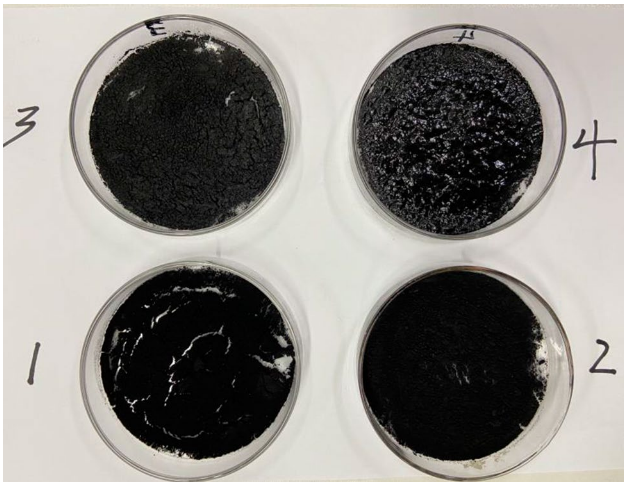

Fig. 11 Physical diagram of composite adsorbents cycle

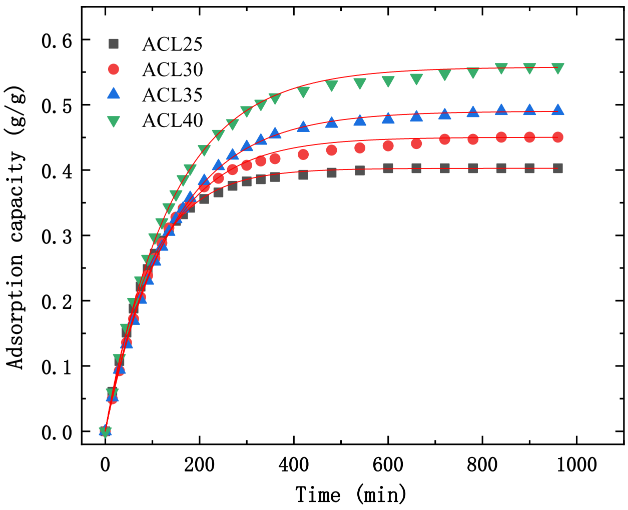

Fig. 12 Adsorption kinetics of composite adsorbents at 25 °C and 45% RH fitting curve

Table 2 Parameters and coefficients related to adsorption kinetic model

Samples	q_e (mg g^{-1})	k (s^{-1})	R^2
ACL25	403	0.011	0.9995
ACL30	450	0.008	0.9978
ACL35	490	0.007	0.9997
ACL40	558	0.007	0.9991

shows the fitting curves of the adsorption kinetics of the composite adsorbents at 25 °C and 45% RH under common environmental conditions, and the result shows that the adsorption data under this condition can be well fitted. It can be seen from Table 2 that the rate coefficient of ACL25 is higher than that of the other three salt contents, and the adsorption equilibrium can be reached in the shortest time, and the adsorption rate of equilibrium water is significantly improved. This is because the hygroscopic salt in the composite adsorbents enter the matrix pores, increasing the diffusion resistance (Zhao et al. 2021). Also, we can see that the composite adsorbents with higher salt content has a stronger water vapor adsorption capacity. However, the number of macropores that can achieve rapid water vapor adsorption is reduced in composite adsorbents with higher salt content, so it takes longer time to reach adsorption equilibrium, resulting in a lower adsorption rate of composite adsorbents (Teo et al. 2017). In addition, the other conditions showed the same type of adsorption isotherms as this common environmental condition, so the other experimental conditions of this experiment are still consistent with the results of this adsorption kinetic fitting analysis.

Conclusion

In this paper, the composite adsorbent ACL was firstly synthesized by a simple method of grinding calcium chloride and activated carbon, which has the characteristics of relatively simple fabrication method, relatively easy production and more suitable for practical application. The microscopic morphology of the composite adsorbent was characterized by scanning electron microscopy, and the results showed that the microscopic morphology of the composite adsorbent was consistent with the adsorption characteristics. The adsorption and desorption performance of the composite adsorbent ACL under relatively low humidity were investigated, and the composite adsorbent showed high adsorption capacity and good desorption rate, and the composite adsorbent showed good cycle stability during the cycle test. This lays the foundation for the application of the composite adsorbent in practical air–water extraction applications. In addition, the equilibrium adsorption capacity of the composite adsorbent can still reach 0.5516 g/g especially under the high temperature and low humidity working condition of 35 °C and 45% RH, which has some reference significance for the selection of composite adsorbent for air extraction in arid and desert areas.

Acknowledgements This study was funded by Huizhong Zhao-National Natural Science Foundation of China (Contract No. 50976073); Huizhong Zhao-Innovation Program of the Shanghai Municipal Education Commission (Contract No. 13ZZ121).

Author contributions HZ contributed to conceptualization, methodology, writing—review and editing. BZ contributed to writing—original draft, data curation, conduct an experiment. YG contributed to writing—review and editing and suggestions on writing methods. FZ contributed to the experimental opinion and formal analysis. YS contributed to the experimental opinion.

Declarations

Conflict of interest The authors declare that they have no known competing financial interests or personal relationships that could have appeared to influence the work reported in this paper.

References

Chan KC, Chao CYH, Sze-To GN, Hui KS (2012) Performance predictions for a new zeolite 13X/CaCl2 composite adsorbent for adsorption cooling systems. Int J Heat Mass Transf 55:3214–3224

Chan KC, Chao CYH, Wu CL (2015) Measurement of properties and performance prediction of the new MWCNT-embedded zeolite 13X/$CaCl_2$ composite adsorbents. Int J Heat Mass Transf 89:308–319

Courbon E, D'Ans P, Permyakova A, Skrylnyk O, Steunou N, Degrez M et al (2017) Further improvement of the synthesis of silica gel and $CaCl_2$ composites: enhancement of energy storage density and stability over cycles for solar heat storage coupled with space heating applications. Sol Energy 157:532–541

El-Ghonemy AMK (2012) Fresh water production from/by atmospheric air for arid regions, using solar energy: review. Renew Sustain Energy Rev 16:6384–6422

Entezari A, Ge TS, Wang RZ (2018) Water adsorption on the coated aluminum sheets by composite materials (LiCl + LiBr)/silica gel. Energy 160:64–71

Hanikel N, Prévot MS, Yaghi OM (2020) MOF water harvesters. Nat Nanotechnol 15:348–355

Huang Y, Yu Q, Li M, Jin S, Fan J, Zhao L et al (2021) Surface modification of activated carbon fiber by low-temperature oxygen plasma: textural property, surface chemistry, and the effect of water vapor adsorption. Chem Eng J 418:129474

Jarimi H, Powell R, Riffat S (2020) Review of sustainable methods for atmospheric water harvesting. Int J Low Carbon Technol 15:253–276

Kim H, Cho HJ, Narayanan S, Yang S, Furukawa H, Schiffres S et al (2016) Characterization of adsorption enthalpy of novel water-stable zeolites and metal-organic frameworks. Sci Rep UK 2016:6

Koc C, Koc AB, Gok F, Duran H (2020) Sustainable water harvesting from the atmosphere using solar-powered thermoelectric modules. Pol J Environ Stud 29:1197–1204

Li R, Shi Y, Wu M, Hong S, Wang P (2020) Improving atmospheric water production yield: enabling multiple water harvesting cycles with nano sorbent. Nano Energy 67:104255

Mesgarian R, Heydarinasab A, Rashidi A, Zamani Y (2020) Adsorption and growth of water clusters on UiO-66 based nanoadsorbents: a systematic and comparative study on dehydration of natural gas. Sep Purif Technol 239:116512

Mohamed MH, William GE, Fatouh M (2017) Solar energy utilization in water production from humid air. Sol Energy 148:98–109

Oladoye PO, Adegboyega SA, Giwa AA (2021) Remediation potentials of composite metal-organic frameworks (MOFs) for dyes as water contaminants: a comprehensive review of recent literatures. Environ Nanotechnol Monitor Manag 16:100568

Salehi AA, Ghannadi-Maragheh M, Torab-Mostaedi M, Torkaman R, Asadollahzadeh M (2020) A review on the water-energy nexus for drinking water production from humid air. Renew Sustain Energy Rev 120:109627

Sharshir SW, Algazzar AM, Elmaadawy KA, Kandeal AW, Elkadeem MR, Arunkumar T et al (2020) New hydrogel materials for improving solar water evaporation, desalination and wastewater treatment: a review. Desalination 491:114564

Srithar K, Rajaseenivasan T (2018) Recent fresh water augmentation techniques in solar still and HDH desalination—a review. Renew Sustain Energy Rev 82:629–644

Sun Y, Spieß A, Jansen C, Nuhnen A, Gökpinar S, Wiedey R et al (2020) Tunable LiCl@UiO-66 composites for water sorption-based heat transformation applications. J Mater Chem A 8:13364–13375

Teo HWB, Chakraborty A, Kayal S (2017) Post synthetic modification of MIL-101(Cr) for S-shaped isotherms and fast kinetics with water adsorption. Appl Therm Eng 120:453–462

Tso CY, Chao CYH (2012) Activated carbon, silica-gel and calcium chloride composite adsorbents for energy efficient solar adsorption cooling and dehumidification systems. Int J Refrig 35:1626–1638

Tu Y, Wang R, Zhang Y, Wang J (2018) Progress and expectation of atmospheric water harvesting. Joule 8:1452–1475

Ur Rehman A, Maosheng Z, Hayat A (2019) Water sorption studies on $ZnSO_4$-zeolite composite as potential thermochemical heat storage materials. Int J Energy Res 44:269–281

Wang JY, Wang RZ, Wang LW (2016) Water vapor sorption performance of ACF-$CaCl_2$ and silica gel-$CaCl_2$ composite adsorbents. Appl Therm Eng 100:893–901

William GE, Mohamed MH, Fatouh M (2015) Desiccant system for water production from humid air using solar energy. Energy 90:1707–1720

Xu C, Yu Z, Xie Y, Ren Y, Ye F, Ju X (2018) Study of the hydration behavior of zeolite-$MgSO_4$ composites for long-term heat storage. Appl Therm Eng 129:250–259

Xu SZ, Wang RZ, Wang LW, Zhu J (2019a) Performance characterizations and thermodynamic analysis of magnesium sulfate-impregnated zeolite 13X and activated alumina composite sorbents for thermal energy storage. Energy (oxford) 167:889–901

Xu JX, Li TX, Chao JW, Yan TS, Wang RZ (2019b) High energy-density multi-form thermochemical energy storage based on multistep sorption processes. Energy 185:1131–1142

Ye H, Yuan Z, Li S, Zhang L (2014) Activated carbon fiber cloth and $CaCl_2$ composite sorbents for a water vapor sorption cooling system. Appl Therm Eng 62:690–696

Yu Q, Zhao H, Sun S, Zhao H, Li G, Li M et al (2019) Characterization of $MgCl_2$/AC composite adsorbent and its water vapor adsorption for solar drying system application. Renew Energy 138:1087–1095

Zhang H, Yuan Y, Yang F, Zhang N, Cao X (2015) Inorganic composite adsorbent $CaCl_2$/MWNT for water vapor adsorption. Rsc Adv 5:38630–38639

Zhang YN, Wang RZ, Li TX (2018) Thermochemical characterizations of high-stable activated alumina/LiCl composites with multistage sorption process for thermal storage. Energy (oxford) 156:240–249

Zhao H, Wang Z, Li Q, Wu T, Zhang M, Shi Q (2020a) Water sorption on composite material "zeolite 13X modified by LiCl and $CaCl_2$. Microporus Mesoporus Mater 299:1–26

Zhao H, Li Q, Wang Z, Wu T, Zhang M (2020b) Synthesis of MIL-101(Cr) and its water adsorption performance. Microporous Mesoporous Mater 297:110044

Zhao H, Zhang Z, Hou H, Zhang J (2021) Hygroscopic salt-modulated UiO-66: synthesis and its open adsorption performance. J Solid State Chem 301:122304